Biosensors and Bioelectronics 26 (2011) 4301–4307

Contents lists available at ScienceDirect

Biosensors and Bioelectronics

journal homepage: www.elsevier.com/locate/bios

A bio-inspired two-layer multiple-walled carbon nanotube–polymer composite sensor array and a bio-inspired fast-adaptive readout circuit for a portable electronic nose

L.C. Wang [a], K.T. Tang [b,*], S.W. Chiu [b], S.R. Yang [b], C.T. Kuo [a]

[a] Department of Materials Science and Engineering, National Chiao Tung University, Taiwan
[b] Department of Electrical Engineering, National Tsing Hua University, No. 101, Sec. 2, Kuang-Fu Road, Hsinchu, Taiwan

ARTICLE INFO

Article history:
Received 25 February 2011
Received in revised form 6 April 2011
Accepted 7 April 2011
Available online 30 May 2011

Keywords:
Electronic nose
Sensor array
Multi-walled carbon nanotube (MWNT)
Adaptive interface

ABSTRACT

We report a fully integrated, portable, battery-operated electronic nose system comprising a bio-inspired two-layer multiple-walled carbon nanotube (MWNT)–polymer composite sensor array, a bio-inspired fast-adaptive readout circuit, and a microprocessor embedded with a pattern recognition algorithm. The two-layer MWNT–polymer composite sensor is simple to operate, and the membrane quality can be easily controlled. These two-layer membranes have improved sensitivity and stability. The fast-adaptive readout circuit responds to the sensor response, while tuning out the long-term constant background humidity, temperature, and odors. This portable electronic nose system successfully classified four complex alcohol samples 40 times for each sample; these samples were sake, sorghum liquor, medical liquor, and whisky.

1. Introduction

An artificial electronic nose (E-Nose) system is a biomimetic system for odor detection, analysis, and recognition. Since it was first developed in 1987 (Gardner et al., 1987), the E-Nose has been adapted for use in a wide range of applications, such as environmental monitoring (Baby et al., 2000; Lamagna et al., 2008), food product quality control (Capone et al., 2000; Balasubramanian et al., 2008; Panigrahi et al., 2006), agricultural evaluation (Gómez et al., 2006; Pathange et al., 2006), the automotive industry (Sobański et al., 2006; Morvan et al., 2000), health management, and medical diagnosis (Pavlou et al., 2002; Lin et al., 2001; Bernabei et al., 2008; D'Amico et al., 2010).

Recent efforts have yielded a miniaturized and inexpensive chemical gas sensor (Guérin et al., 2005; Tang et al., 2006; Yamaguchi and Yang, 2004) with high reproducibility and a rapid reaction rate. Research, including that from our own group, working under size and price restraints, has produced a portable E-Nose based on a carbon black–polymer composite sensor array (Kim et al., 2005; Matzger et al., 2000). Compared those of with carbon black, the electrical conduction properties of carbon nanotubes (CNTs) have drawn considerable interest (Grant and White, 1991; Park et al., 2009), and multiple-walled carbon nanotube (MWNT)–polymer composite sensors show very good performance with respect to sensitivity, response time, reproducibility, and long-term stability (Wu and Lin, 2006; Alig et al., 2007).

To improve sensor performance further, researchers have studied biological olfaction as a reference. Mammalian olfactory receptor cells distributed in the olfactory epithelium contain a mucous covering layer. The surface of an olfactory cell consists of tens of cilia, which extend into the mucus. As gas molecules enter the nose, they first dissolve in the mucus before being captured by the cilia. The mucus filters out dust and impurities that could otherwise damage the cilia. The receptor cells then transmit neural signals to the cerebrum. This two-layer structure inspired researchers to investigate the use of artificial mucosa to emulate this mechanism, and the use of artificial mucosa resulted in a five-fold increase in sensitivity (Gardner et al., 2007). The artificial mucosa approach uses GC columns with a 10 mm thick layer of Parylene C (polymonochloroparaxylylene C) to emulate the mucosa and 40 polymer-composite sensors to emulate the cilia. We were inspired by the biological two-layer structure in a different way. Traditional conducting polymer sensors mix conducting materials (such as carbon black, CNTs, SWNTs, and MWNTs) and polymers into one sensing film layer. Inspired by the olfactory structure, we created a two-layer film in which polymer and conducting materials are two different layers. Test results for the new device verified that this approach results in a higher sensing performance than the traditional single-layer film process.

* Corresponding author. Tel.: +886 3 5162178.
E-mail address: kttang@ee.nthu.edu.tw (K.T. Tang).

0956-5663/$ – see front matter © 2011 Elsevier B.V. All rights reserved.
doi:10.1016/j.bios.2011.04.015

For resistive type sensors, the readout circuit provides either a varying sensor voltage at a constant current or a variable sensor current at a constant voltage; thus, use of a Wheatstone bridge is commonplace. However, MWNT–polymer composite sensor circuits suffer from severe interference resulting from sensitivities to water vapor, temperature, and background odors, which result in a low signal-to-noise ratio. Furthermore, the sensors may not return to the original baseline at the end of each sensing cycle.

To overcome these problems, we devised a "bio-inspired fast-adaptive readout circuit." Phasic receptors in biological systems adapt rapidly to a stimulus. The response diminishes very quickly and then ceases. The olfactory receptor is one example that adapts rapidly to an odor stimulus. The readout circuit responds to the sensor response signal while tuning out long-term, constant signals from background humidity, temperature, and odors.

Using a two-layer MWNT–polymer composite sensor array, together with a fast-adaptive readout circuit and a microprocessor containing a pattern recognition algorithm, we produced a portable E-Nose system. The remainder of this paper consists of three sections: Section 2 describes the sensor, the interface circuit, and the experimental setup; Section 3 presents the experimental results for the sensors and the assembled portable E-Nose system and the system's performance in the detection of four different alcohols as test samples; and Section 4 concludes this manuscript.

2. Experimental

2.1. MWNT–polymer gas sensor-array chip

The MWNT–polymer gas-sensor array chip has twelve independent sensing areas on a single silicon substrate (Chang et al., 2004; Chang and Yuan, 2009). Ten sensor array chips were fabricated on a 4-inch Si wafer using the batch process, and each sensor chip was 34 mm × 20 mm in area. Eight of the sensing areas were coated with sensing components, while the remaining four areas were reserved for future addition of a humidity sensor, two temperature sensors, and a heating device to provide greater control and stability of the sensing system. Each sensing element contained a circular membrane with a diameter 2 mm to minimize heat loss from the silicon substrate.

The polymers were selected according to two processes: the linear solvation energy relationship (LSER) theory, and physical absorption bonding. The first process is applying the LSER theory to enhance the device's recognition capability for different odors (Grate et al., 1995, 1999). LSER equations correlate the log of the partition coefficient of a vapor in a polymer with the vapor solvation parameters using a series of LSER coefficients related to the polymer's solubility properties.

For example, applying LSER equation to estimate the solvation coefficient between ethanol gas and various polymer membranes, and considering parameters such as dispersive interactions, dipole interactions, hydrogen bond acidity, and hydrogen bond basicity, we can estimate the solvation coefficients as PMVEMA < PEA < HPMC < PVBC. A smaller solvation coefficient corresponds to a larger interaction between ethanol gas and polymer, resulting in a larger resistance variation. Therefore, solvation coefficient provides a good estimation.

However, carbon nanotubes may change the physical characteristics of the film (glass transition temperature, rigidity, and density), and possibly the chemical characteristics. Therefore, solvation energies may not be sufficient for complete description of the sensor–analyte interaction.

When using carbon nanotube–polymer composites as gas sensors, to use the sensors repetitively with a short recovery time, the interaction between the gas and polymer membrane is usually reversible physical absorption bonding. There are five kinds of physical absorption bonding: (1) hydrogen-bond acidic (HBA), (2) hydrogen-bond basic (HBB), (3) dipolar and hydrogen-bond basic (D-HBB), (4) moderately dipolar and weakly H-bond basic or acidic (MD-HB), and (5) weakly dipolar with weak or no hydrogen-bond properties (WD) (Ryan et al., 1998; Hierlemann et al., 2001).

Consequently, we selected eight polymer materials. These were styrene/allyl alcohol copolymer (SAA) (WD), polyvinylpyrrolidone (PVP) (HBB), poly(vinylidene chloride-co-acrylonitrile) (P(VDC-AN)), poly(methyl vinyl ether-alt-maleic acid) (PMVEMA), poly(alpha-methylstyrene)(PMS) (WD), hydroxypropyl methyl cellulose (HPMC) (D-HBB), poly(ethylene adipate) (PEA) (HBA), and poly(vinyl benzyl chloride) (PVBC) (D-HBB).

We adopted two different methods to fabricate the gas-sensing films for these sensors:

(1) One-layer film-making method: the selected polymers were dissolved in methyl ethyl ketone (MEK) solvent, and MWNTs (1 wt.%) were added. The mixture was magnetically stirred under ultrasonic oscillation to achieve uniform dispersion. The uniformly mixed composite precursor was injected onto the chip using an HPLC syringe. The solvent was removed, and the composite membrane formed by baking in a vacuum oven for 24 h.
(2) Two-layer film-making method: a MWNT-modified electrode layer was prepared by drop-casting 1 mg/ml MWNTs (1 wt.%) dispersed in MEK onto the surface of an interdigitated microelectrode (IME) device. The MEK solvent was evaporated in air, at room temperature, to yield the MWNT film. The polymer films were deposited by drop casting their solutions onto the MWNT layer, followed by drying *in vacuo*, to form the multilayer films.

2.2. Fast-adaptive readout circuit

Fig. 1a shows the integrated printed circuit board (PCB) interface with the eight adaptive interface circuits, an eight-to-one multiplexer (MUX), and an 8-bit analog-to-digital converter (ADC). The interface PCB forms a bridge between the eight-channel sensor array chip and the microprocessor. The eight adaptive interface circuits connect with eight different sensors. Fig. 1b shows the schematic of the adaptive interface circuit. The circuit has two operating modes. Mode-1, Calibration mode: Prior to sensing odors, the multiplexer (MUX) chooses path "1″ to charge the capacitor, C_{FB}, and control the gate voltage of transistor M_N. This forces the voltage (V_{adpt}) to become equal the reference voltage, V_{REF}, as a baseline signal. In this mode, the n-channel metal–oxide–semiconductor field-effect (NMOS) transistor M_N operates as a voltage-controlled current source. Mode-2, odor-sensing mode: to sense odors, the MUX chooses path "0″. The NMOS gate voltage has long-duration hold capabilities to maintain a steady I_{Mn} because of the large time constant $R_{FB}C_{FB}$. In this mode, the sensor resistance change converts to a voltage change of V_{adpt} by Ohm's law.

The novelty of this circuit is that the circuit operates in two modes with different time constants, one is very small and the other one is very large. This is the most important bio-inspiration feature of the circuit. For the biological nose, when encountering a new odor stimulus, it first responds very quickly, and then adapts to the odor. This feature helps the biological nose to detect the next new odor stimulus quickly, even if the original odor stimulus still exists in the environment. In addition, this feature helps to ignore the background parameters such as temperature and humidity. We have implemented this feature in the bio-inspired fast adaptive readout circuit. Since the baseline resistances of various sensors are different, the calibration mode brings the circuit to an appropriate bias condition quickly with a small time constant. Then the

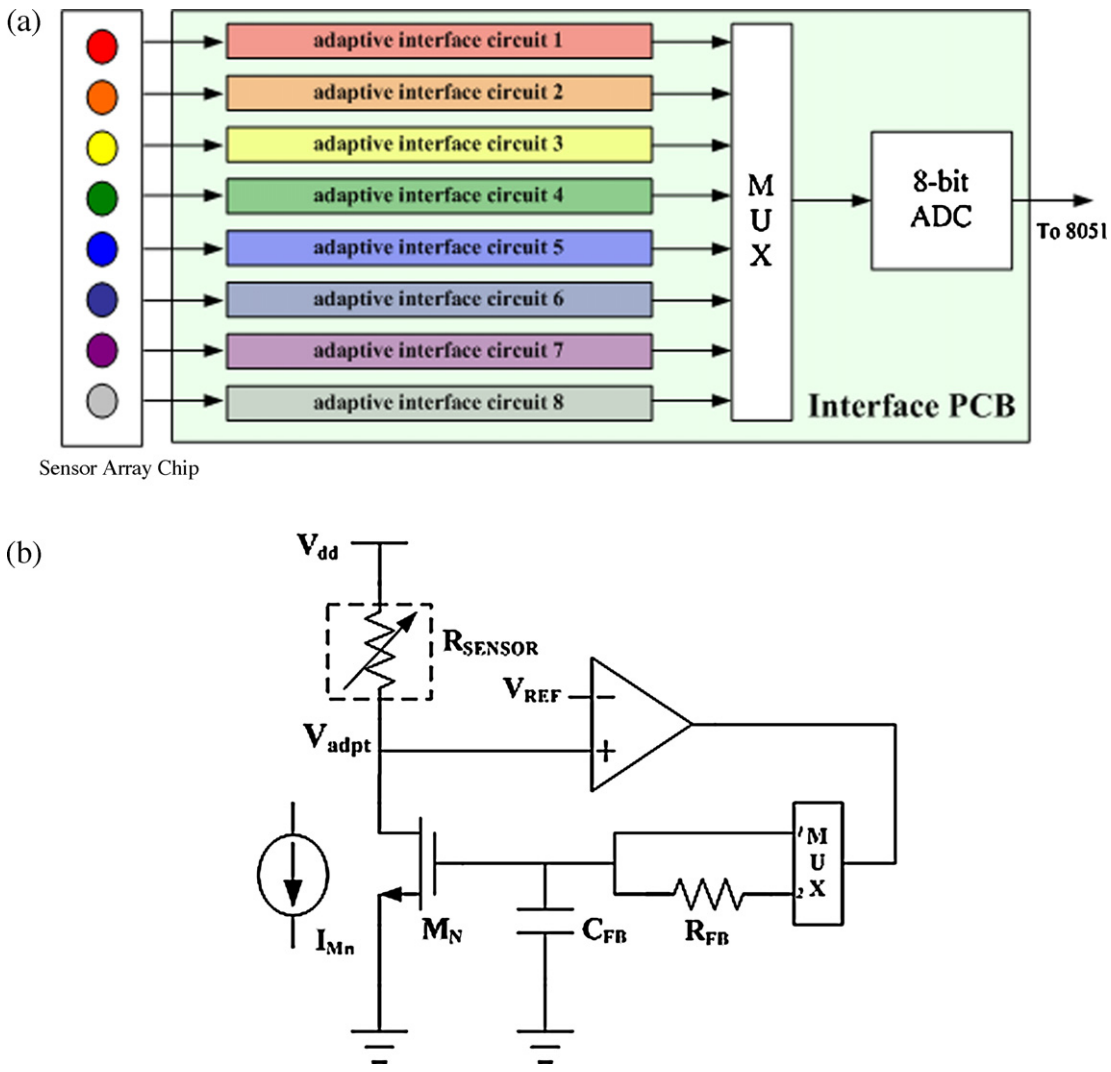

Fig. 1. (a) Block diagram of the interface PCB, and (b) schematic of the adaptive interface circuit.

circuit switches to odor-sensing mode operating with a long time constant in the feedback loop. When encountering a new odor stimulus, the circuit responds quickly, and then adapts to the odor, just like the biological nose. In addition, the circuit tunes out the long time-constant parameters for background humidity, temperature, and odors. After each sensing cycle, the circuit returns to its baseline through the slow adaptation.

Eqs. (1) and (2) provide the sensing voltage, V_{adpt}, for the calibration and odor-sensing modes, respectively:

$$V_{adpt.Calibration} = V_{dd} - R_{SENSOR} I_{Mn} \quad (1)$$

$$V_{adpt.Odor} = V_{dd} - (R_{SENSOR} + \Delta R_{SENSOR}) I_{Mn} \quad (2)$$

The sensing voltage signal feeds into an ADC through an eight-to-one MUX, for conversion into a digital signal. The output is forwarded to the microprocessor for further signal processing. Only one ADC is required for the interface PCB in odor-sensing mode because the adaptive interface circuit outputs a signal with a long time constant; the requirement for only a single ADC reduces power consumption and area costs. After receiving the sensor signals from the ADC, the microprocessor calculates the resistance change ratio according to Eq. (3):

$$\frac{\Delta R_{SENSOR}}{R_{SENSOR}} = \frac{V_{adpt.Calibration} - V_{adpt.Odor}}{V_{dd} - V_{adpt.Calibration}} \quad (3)$$

Because $V_{adpt.Calibration}$ and V_{dd} are acquired in calibration mode, the microprocessor needs to acquire only $V_{adpt.Odor}$ when in the odor-sensing mode, thus decreasing the microprocessor signal-processing load. The resistance change ratios ($\Delta R_{SENSOR}/R_{SENSOR}$) for the eight sensor resistances, as calculated by the microprocessor, form an odor pattern for the input odor. This pattern is processed further according to one of the operational modes (training mode and testing mode). In the training mode, the odor pattern is stored to the database. In the testing mode, an embedded K-nearest neighbor (KNN) pattern recognition algorithm identifies the odor pattern, and results appear on a liquid crystal display (LCD).

2.3. Experimental setup

Fig. 2 shows the experimental setup used to characterize the volatile organic compound (VOC)-sensing properties of the sensor devices. To perform the experiments, the sensor device was placed in a glass testing chamber. The analyte vapor flow was controlled by a calibrated Aalborg mass-flow controller (GFM-17), and the flow rate of the vapor stream was maintained at 100 mL/min. We used a KIN-TEK 670C Standard Gas Generator (KIN-TEK, Laboratories, Inc.) as our vapor-generating system. The vapor stream was produced by evaporation of a volatile solvent and using the controller to manipulate the vapor concentration. A constant heater was used

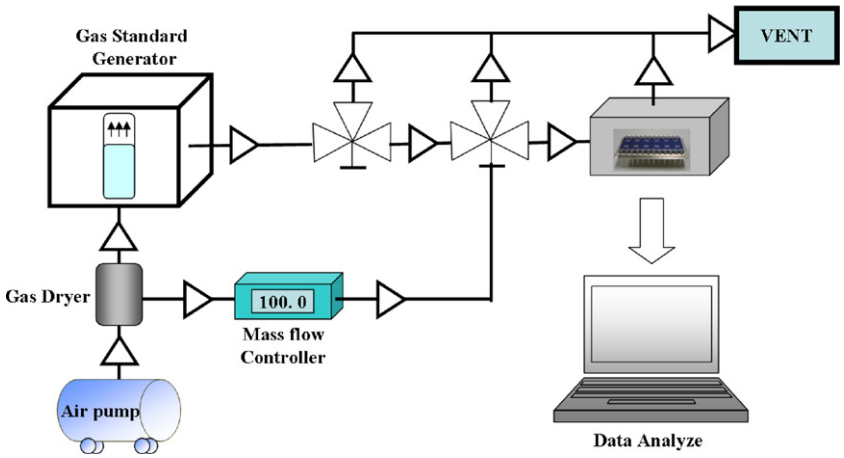

Fig. 2. The experimental setup used to characterize the sensing volatile organic compound (VOC).

to increase the temperature in the tube to evaporate the organic solvent. After the system reached a steady state with respect to temperature and flow rate, the testing gas attained a stable concentration. In theory, the temperature setting can control the diffusion rate, and the vapor concentration can be accurately determined by measuring the weight loss from the organic solvent. The test gas was carried by a stream of air provided by an air compressor, and the gas flow was managed by the mass flow controller. The target gas was directed into the glass testing chamber containing the sensor array. For each test, the target gas was infused into the chamber for 300 s (adsorption), and then dry air was infused for another 600 s (desorption). After completion of each experimental run, the chamber was purged with dry air. The sensor's electrical resistance outputs were measured using a digital multimeter with signals addressed by a multiplexer switch unit. The sensor array signals were sent to the remainder of the E-Nose system, outside of the chamber, for signal manipulation and odor classification.

3. Results and discussion

3.1. Fabrication of MWNT–polymer membranes by one-layer and two-layer methods

We prepared MWNT–polymer composite membranes using one-layer and two-layer methods, and we then performed odor-sensing experiments. After exposing the membranes to methanol, the array resistances were measured. Fig. 3a and b shows scanning electron microscope (SEM) micrographs of the surface of the different sensing membranes. The sensing surface produced by the one-layer method includes many MWNTs, while the sensing

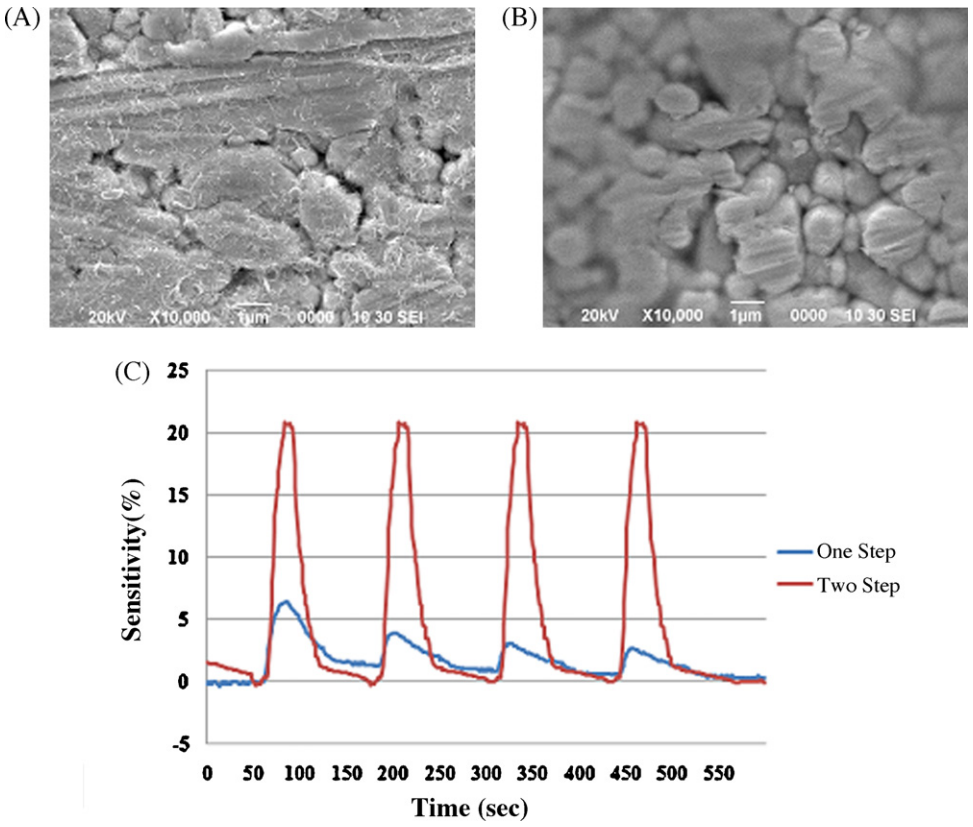

Fig. 3. (a and b) The SEM of the surface of the different sensing membranes and (c) the electric sensing characteristics of the two different membranes.

surface produced by the two-layer method shows only polymer, with no MWNTs visible. This result suggests that MWNTs disrupt the one-layer sensing membrane. On the other hand, in the two-layer sensing membrane, only the polymer layer contacts the test gas, and the MWNTs serve only as a conducting layer, reducing their interference when sensing gases.

The one-layer and two-layer sensing films were placed in the same chamber to conduct gas experiment at the same time to compare their performances. For each test, the flow rate of the vapor stream was maintained at 100 mL/min. We set the KIN–TEK gas generator at 40 °C. Methanol gas (3.7%, v/v) was first infused into the chamber for 40 s (adsorption), and then dry air was infused for another 90 s (desorption). The experiment was repeated four times. Fig. 3c shows the gas test results of the one-layer and two-layer sensing films. Under the same experimental conditions, the two-layer membrane has a better performance than the one-layer membrane with respect to three factors: (1) higher sensitivity: the two-layer membrane has a sensing response at 20.5%, while the one-layer membrane has a maximum sensing response at 6%. (2) Faster recovery time: although these two membranes have similar response times, the two-layer membrane has a recovery time of 30 s, while the one-layer membrane's recovery time is 60 s. (3) Better repeatability: according to Fig. 3c, the two-layer membrane can be used at least four times with similar performance, while the sensor response magnitude of the one-layer membrane degrades with additional tests.

The principle of the conducting-polymer type gas sensor is that the polymer membrane absorbs gas, swells, and causes a resistance change. Because the top level of the two-layer film is only polymer, the polymer is in direct contact with target gas, resulting in faster absorption and desorption. In addition, this polymer-only layer has a higher surface area with which to make contact with the target gas, resulting in a larger response. In contrast, a portion of the surface area of the one-layer film is occupied by CNTs, and thus it has a smaller response. In addition, because CNTs blocks some of the polymer pores (or free volume), the diffusion length of the target gas in the polymer is longer, resulting in a longer desorption time.

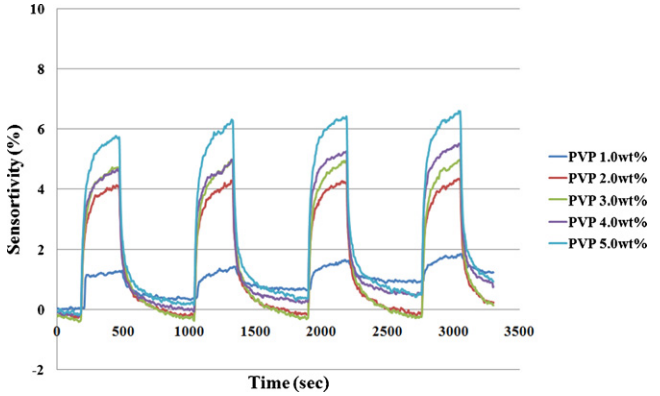

Fig. 4. Gas sensing responses of MWNT–polymer (PVP) composite films with different polymer concentrations to ethanol gas.

In summary, the two-layer membrane has a higher sensitivity, faster recovery time, and better repeatability. Consequently, we adopted the two-layer method for fabrication of our composite sensing materials.

3.2. Fabricating composite membranes with various MWNT–polymer ratios

After preparing the 1 wt.% MWNT conductive layer, various concentrations (1.0 wt.%, 2.0 wt.%, 3.0 wt.%, 4.0 wt.%, and 5.0 wt.%) of polyvinylpyrrolidone (PVP) solution were used to prepare the MWNT–polymer membranes. These five membranes were exposed to ethanol vapors (Fig. 4). After ethanol absorption, the 2.0, 3.0, and 4.0 wt. % PVP membrane resistances gradually increased, reached maximum at 20 s, and remained stable at around 4% resistance change. The 1.0 wt.% PVP membrane reached its maximum change over a similar time scale as that of the lower PVP content devices, with a 1% change in resistance. The 5.0 wt.%

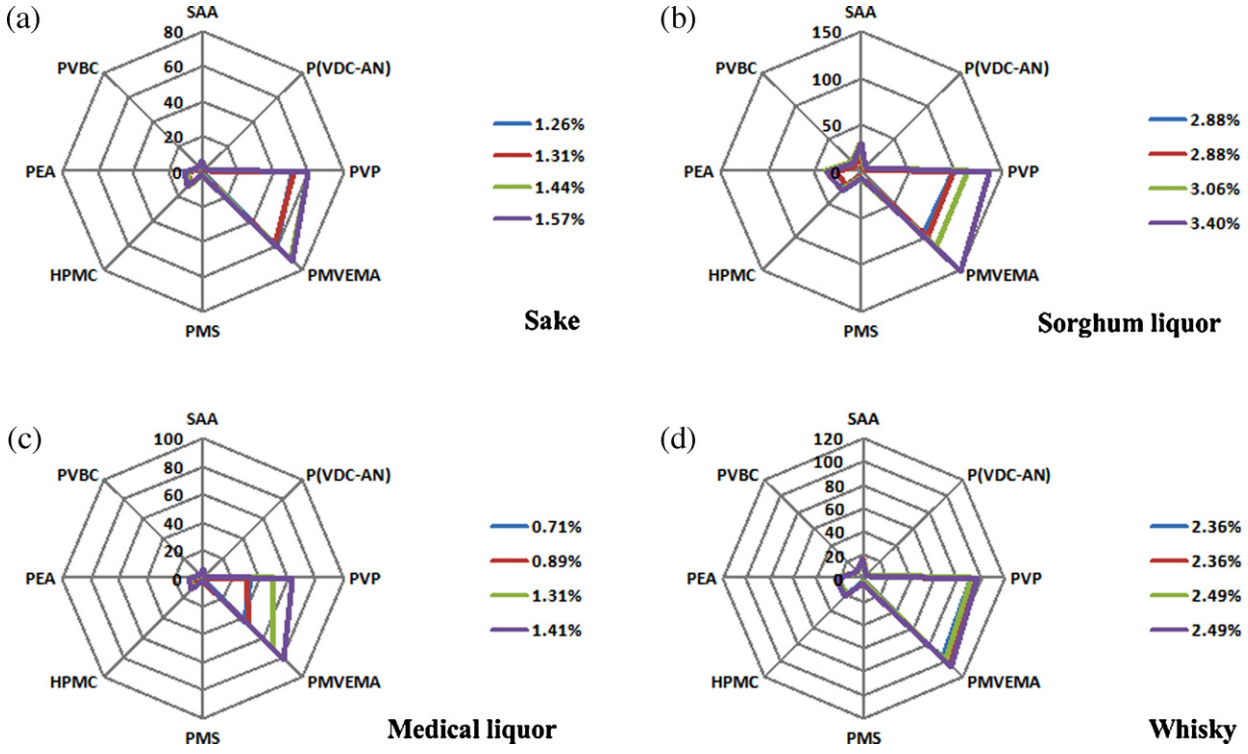

Fig. 5. Radar plots with different concentration of (a) sake, (b) sorghum liquor, (c) medical liquor, and (d) whisky.

PVP membrane produced a fast and large response, reaching a maximum 6% change in resistance within 20 s.

Although the higher concentration (4.0 wt.% and 5.0 wt.%) PVP membranes produced the fastest and largest responses among the five sample membranes, some polymers did not have a higher solubility in the solvent, and some polymers at 4–5 wt.% were very sticky and difficult to introduce into a micropipette. Therefore, we used lower concentration polymer formulations (1–3 wt.%) to produce MWNT–polymer membranes for the sensing experiments described below.

3.3. Sensor array chip response

Fig. 5 shows radar plots of the four complex alcohol odors (sake, sorghum liquor, medical liquor, and whisky). The magnitude for each axis was obtained by Eq. (3). As expected, the four patterns were very similar because the four alcohol odors have similar chemical compositions. In addition to the patterns, the figures also show that the sensor response increased with increasing odor concentration. In summary, the sensor array chip shows the desirable characteristics of rapid response time and high reproducibility, suggesting its suitability for the proposed portable E-Nose system.

3.4. The portable E-Nose system

To assemble the portable E-Nose system, a dedicated sensor readout and data acquisition electronics were implemented on a PCB to eliminate the use of a bulky and heavy digital apparatus, such as a laptop personal computer (PC). The microprocessor embeds a k-nearest neighbor (KNN) classification algorithm for simplicity to achieve a good efficiency and performance (Tang et al., 2010). Fig. 6a and b shows the fully integrated portable E-Nose system. Its dimensions are 28 cm × 18 cm × 12 cm, and its weight is 540 g. The portable E-Nose has a very low power consumption and is capable of running for several hours with only two batteries. The classification results are shown on an LCD.

The fully integrated portable E-Nose system was tested with four complex alcohol odors (sake, sorghum liquor, medical liquor, and whisky) to evaluate its performance. Ten data points for each odor were taken as a training database for the system. After training the system, each of the four odors was applied to the system thirty times. Fig. 6c shows the three-dimensional projection of the principle component analysis (PCA) results. The dashed ellipsoids in the figures show the clear recognition boundaries of the four odors. Supplementary Material Table 1 shows the classification accuracy of the three KNN-based algorithms (KNN, linear

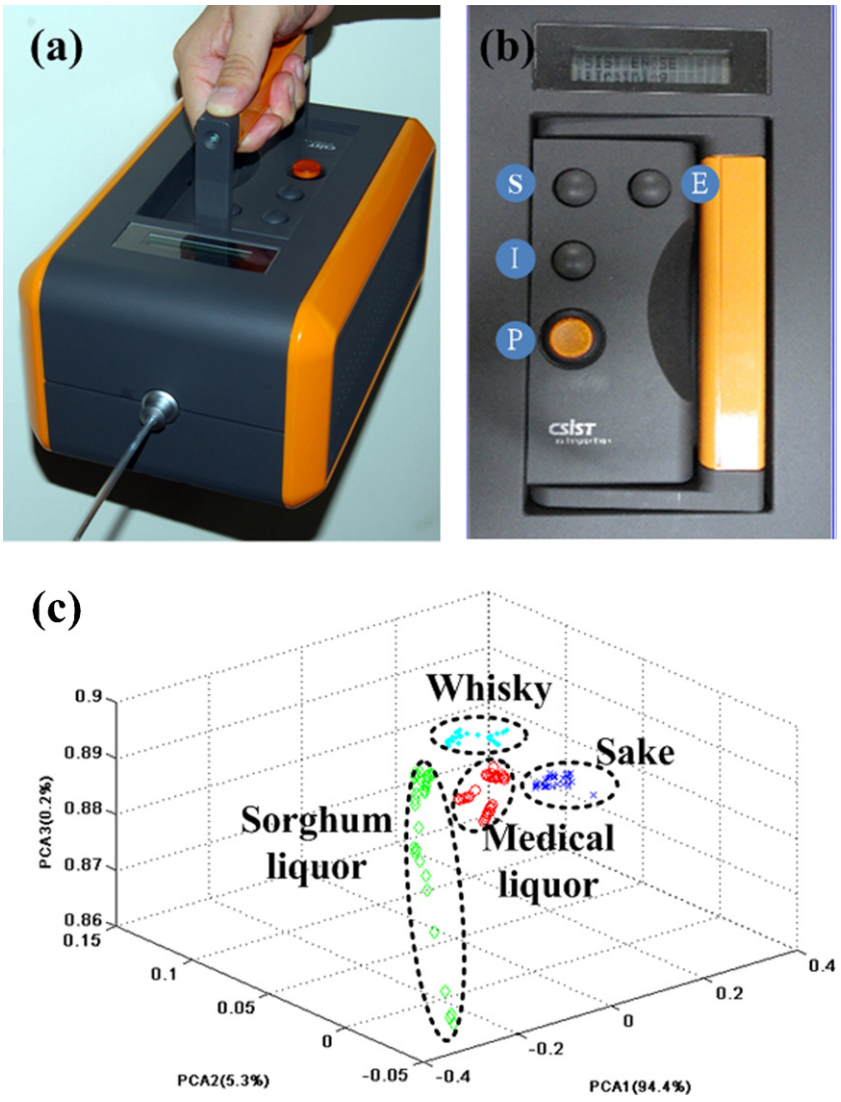

Fig. 6. (a) The fully integrated portable E-Nose system, (b) control interface of the portable E-Nose (P: power On/Off, I: E-Nose system initialization, S: training/testing mode selection, and E: enter), and (c) the three-dimensional projection of the PCA results.

discriminant analysis (LDA)+KNN and PCA+KNN), where all three KNN-based algorithms have high accuracy (over 95% for $K \leq 3$). The portable E-Nose system implemented the KNN algorithm in the 8051 microprocessor, selected for its simplicity, as compared to the other two algorithms, in order to achieve the best efficiency and performance. Although the odor patterns for these four complex odors were alike because of their similar chemical compositions, the portable E-Nose system successfully classified each complex alcohol odor, verifying the correct operation of the portable E-Nose system.

4. Conclusions

We fabricated a conductive MWNT–polymer two-layer composite material inspired by the structure of the olfactory system. Through a combination of conducting MWNTs and a sensing polymer, this material provided enhanced sensitivity, making it highly suitable as a microarray gas-sensing element. The sensor response was read by a bio-inspired fast-adaptive circuit, which tuned out long-term time constant background signals resulting from humidity, temperature, and other non-test odors. The sensor array and readout circuit were fabricated together with a microprocessor to form a portable E-Nose system. The portable E-Nose successfully identified four similar complex alcohol vapors: sake, sorghum liquor, medical liquor, and whisky; each alcohol was tested 40 times. This research should prove very helpful for future development of integrated gas-sensing "system-on-chip (SoC)" designs.

Acknowledgments

The authors would like to acknowledge the support of the National Science Council of Taiwan, under Contract No. NSC 97-2220-E-007-036 and NSC 98-2220-E-007-017. We also acknowledge the support of the Chung-Shan Institute of Science and Technology, under Contract No. CSIST-808-V207. We also thank the National Chip Implementation Center and Prof. C.P. Chang, National Deference University for technical support.

Appendix A. Supplementary data

Supplementary data associated with this article can be found, in the online version, at doi:10.1016/j.bios.2011.04.015.

References

Alig, I., Lellinger, D., Dudkin, S.M., Pötschke, P., 2007. Polymer 48, 1020–1029.
D'Amico, A., Pennazza, G., Santonico, M., Martinelli, E., Roscioni, C., Galluccio, G., Paolesse, R., Natale, C.D., 2010. Lung Cancer 68, 170–176.
Baby, R.E., Cabezas, M., Reca, E.N.W.d., 2000. Sens. Actuators B: Chem. 69, 214–218.
Balasubramanian, S., Panigrahi, S., Logue, C.M., Doetkott, C., Marchello, M., Sherwood, J.S., 2008. Food Control 19, 236–246.
Bernabei, M., Pennazza, G., Santonico, M., Corsi, C., Roscioni, C., Paolesse, R., Natale, C.D., D'Amico, A., 2008. Sens. Actuators B: Chem. 131, 1–4.
Capone, S., Siciliano, P., Quaranta, F., Rella, M.E.R., Vasanelli, L., 2000. Sens. Actuators B: Chem. 69, 230–235.
Chang, C.-P., Chao, C.-Y., Huang, J.H., Li, A.-K., Hsu, C.-S., Lin, M.-S., Hsieh, B.R., Su, A.-C., 2004. Synth. Met. 144, 297–301.
Chang, C.-P., Yuan, C.-L., 2009. J. Mater. Sci. 44, 5485–5493.
Gardner, J.W., Bartlett, P.N., Dodd, G.H., Shurmer, H.V., 1987. 8th Int. Congress of European Chemoreception Research Organisation , University of Warwick, UK.
Gardner, J.W., Covington, J.A., Tan, S.-L., Pearce, T.C., 2007. Proc. R. Soc. A 463, 1713–1728.
Gómez, A.H., Hu, G., Wang, J., Pereira, A.G., 2006. Comput. Electron. Agric. 54, 44–52.
Grant, E.R., White, M.G., 1991. Nature 354, 249–250.
Grate, J.W., Patrash, S.J., Abraham, M.H., 1995. Anal. Chem. 67, 2162–2169.
Grate, J.W., Wise, B.M., Abraham, M.H., 1999. Anal. Chem. 71, 4544–4553.
Guérin, J., Aguir, K., Bendahan, M., Lambert-Mauriat, C., 2005. Sens. Actuators B: Chem. 104, 289–293.
Hierlemann, A., Zellers, E.T., Ricco, A.J., 2001. Anal. Chem. 73, 3458–3466.
Kim, Y.S., Ha, S.-C., Yang, Y., Kim, Y.J., Cho, S.M., Yang, H., Kim, Y.T., 2005. Sens. Actuators B: Chem. 108, 285–291.
Lamagna, A., Reich, S., Rodríguez, D., Boselli, A., Cicerone, D., 2008. Sens. Actuators B: Chem. 131, 121–124.
Lin, Y.-J., Guo, H.-R., Chang, Y.-H., Kao, M.-T., Wang, H.-H., Hong, R.-I., 2001. Sens. Actuators B: Chem. 76, 177–180.
Matzger, A.J., Lawrence, C.E., Grubbs, R.H., Lewis, N.S., 2000. J. Comb. Chem. 2, 301–304.
Morvan, M., Talou, T., Gaset, A., Beziau, J.F., 2000. Sens. Actuators B: Chem. 69, 384–388.
Panigrahi, S., Balasubramanian, S., Gu, H., Logue, C., Marchello, M., 2006. LWT – Food Sci. Technol. 39, 135–145.
Park, Y., Dong, K.-Y., Lee, J., Choi, J., Bae, G.-N., Ju, B.-K., 2009. Sens. Actuators B: Chem. 140, 407–411.
Pathange, L.P., Mallikarjunan, P., Marini, R.P., Keefe, D.V., Sean, O', 2006. J. Food Eng. 77, 1018–1023.
Pavlou, A.K., Magan, N., McNulty, C., Jones, J.M., Sharp, D., Brown, J., Turner, A.P.F., 2002. Biosens. Bioelectron. 17, 893–899.
Ryan, M.A., Homer, M.L., Buehler, M.G., Manatt, K.S., Lau, B., Karmon, D., Jackson, S., 1998. Proceedings of the 28th International Conference on Environmental Systems , Danvers, MA.
Sobański, T., Szczurek, A., Nitsch, K., Licznerski, B.W., Radwan, W., 2006. Sens. Actuators B: Chem. 116, 207–212.
Tang, H., Yan, M., Zhang, H., Li, S., Ma, X., Wang, M., Yang, D., 2006. Sens. Actuators B: Chem. 114, 910–915.
Tang, K.-T., Lin, Y.–S., Shyu, J.M., 2010. Sensors 10 (11), 10467–10483.
Wu, T.-M., Lin, Y.-W., 2006. Polymer 47, 3576–3582.
Yamaguchi, N., Yang, M., 2004. Sens. Actuators B: Chem. 103, 369–374.

L.C. Wang received the BS from Department of Chemistry, National Cheng Kung University, Tainan, Taiwan, and received the MS from Department of Chemistry, National Sun Yat-san' University and is currently working for the PhD degree in the Department of Materials and Engineering, National Chiao Tung University, Hsinchu, Taiwan. His main fields of research are application of carbon nanotubes and chemical sensor.

K.T. Tang received his BS from Department of Electrical Engineering, National Taiwan University, Taipei, Taiwan, and received his MS and PhD from Department of Electrical Engineering, California Institute of Technology, Pasadena, CA, USA, in 1998 and 2001. He then joined Second Sight Medical Products Inc. Sylmar, CA, USA as a senior electrical engineer working on retinal prosthesis, from 2001 to 2006. Since 2006, he has joined the Department of Electrical Engineering, National Tsing Hua University, Hsinchu, Taiwan as an assistant professor. His research fields include analog and mixed signal IC design, neuromorphic SoC design, and biomedical SoC design.

S.W. Chiu received the BS (2007) degree from Department of Electrical Engineering, National Central University, Jhongli, Taiwan, and received the MS (2009) degree from department of Electrical Engineering, National Tsing Hua University, Hsinchu, Taiwan, where he is currently working for the PhD degree. His research field is biomedical SoC design.

S.R. Yang received the BS from Department of Chemical Engineering, the National Chun Sing University, Taichung, Taiwan, and received the MS from Department of Chemical Engineering, National Cheng Kung University, Tainan, Taiwan. He is currently working for the PhD degree in Department of Electrical Engineering, National Tsing Hua University, Hsinchu, Taiwan. His main fields of research are analog and mixed signal interface circuits for sensors.

C.T. Kuo received his BS from Department of Material Engineering, National Cheng Kung University, Tainan, Taiwan, and received his MS and PhD from Department of Materials Engineering, University of Maryland, MD, USA, in 1973 and 1977. He is currently professor in the Department of Materials and Engineering, National Chiao Tung University, Hsinchu, Taiwan. His research is focused on the synthesis and applications of nanomaterials, nanostructured oxide materials and nanocomposite materials.